ISSN 1846-6168 (Print), ISSN 1848-5588 (Online)
https://doi.org/10.31803/tg-20240808075046

Original scientific paper
Received: 2024-08-08, Accepted: 2025-04-15

Study the Differential Cross-Section of Scattering Potential (Yukawa, Coulomb and Square Well) around PEMFC

Saddam Husain Dhobi*, Kishori Yadav, Suresh Prasad Gupta, Jeevan Jyoti Nakarmi, Ajay Kumar Jha

Abstract: The objective of this work is to study the differential cross section (DCS) around-surface the electrode of proton exchange membrane (PEMFC) for stability and performance of PEMFC. For this considered a system of electrons proton and hydrogen particle around electrode formed around-surface electrode due to inlet of H_2 and O_2 in PEMFC system. After the particle formed around they go interaction and the region of interaction is defined by S-matrix theory. S-matrix formulation was formulated by Kroll and Watson (1973) for a low-frequency response. After formulation of DCS was calculated for possible three case around electrode of PEMFC. The three case is consideration of Yukawa potential, Coulomb potential and square well potential was calculated found that the DCS of Yukawa potential is less than coulomb potential, and coulomb potential DCS is less than the square well potential at the same interaction strength. The DCS for considered potential in this work ranges widely 10^{-10} a. u. to 1.4×10^{8} a. u. The DCS was studied for both electron and meson at an ideal using square well potential and found that the DCS for meson is greater than an electron, this is because of mass of meson is greater than an electron. The DCS found stable in higher energy range and higher scattering angle indicate system of PEMFC is stable and this may imply to remove the complexity and stability of PEMFC system when the system of PEMFC single cell is design with consideration of DCS and diffusion angle of inlet fuel inside PEMFC.

Keywords: Coulomb potential and square well potential; DCS; Kroll and Watson; PEMFC; S-Matrix; Yukawa potential

1 INTRODUCTION

Electron was discovered by J. J. Thompson in 1897 AD and discovery help the development of physics beyond classical physics. Elastic scattering of alpha particles with foil led to the discovery of the nucleus by Rutherford in 1911 AD. In addition, the discovery also led to the development of the planetary model of the atomic structure. Bohr proposed a model of hydrogen in 1912 AD which also led to the development of new laws and formulation in the field of physics with the assumption that electron in a hydrogen atom moves in a circular orbit due to the Coulomb force between the electron and the nucleus with quantization of angular momentum of the electron and emitter of radiation when electron jump from higher to lower quantum number. A scattering experiment in 1923 AD by Compton [1-5] confirm the existence of photons and the experiment was verified and supported by Bothe and Geiger [6].

One of the most studied phenomena of laser-atom interaction is that of photo-ionization. In photoionization, an electron is removed from a parent atom or ion living behind a single or multiply charged ion. At conventional intensities, only one photon is absorbed in an elementary event of the interaction of light with substance. The energy $\hbar\omega$ of the photon coincides with the difference between the energy levels of the relevant atom [6, 7]. At high intensities of laser, two or more photons may be absorbed in an elementary event of interaction. In this case, light not only the frequency ω but also of the frequencies $\frac{\omega}{2}$, $\frac{\omega}{3}$ etc. may be absorbed. Such absorption is called multi-photon (2 photons, 3 photons, etc.), in this case, the electric field strength is nearly equal to the microscopic field of the atom and optical property depends upon both frequency and intensity (nonlinear case).

The multi-photon ionization for a field is the transition of electrons from a bound state to a continuum state by the simultaneous absorption of more than two photons. This theory based on the scattering method was realized in 1960 AD but Kroll and Watson in 1973 AD [8] gave a new approach to S-matrix for low-frequency response for the solution of the scattering process. It can be extended not scattering but another type of process also. S-matrix formulation was invented in a search for a general non-perturbative formulation to use for strong field problems. It is a suitable approach for free-free scattering it is a suitable approach also for ionization (bound free, recombination free bound and excitation/DE excitation) [9]. The s-matrix method is more useful than another method because this formulation avoids the decoupling problem (nor loss, nor gain of energy due to a very short time).

In this method, the interaction is turned on or off is not absorbable while other methods suffer from this complication [9] S-matrix formulation can be formulated entirely in terms of quantity measurable in the laboratory. It can be applied to any process as long as the space-time domain of the interaction region is bounded. It gives unambiguous rules gauge transformation. S-matrix is related to T-matrix which helps to determine the differential cross-sectional area when electron interacts with the target atom in laser field.

The DCS in the presence of a weak laser field during inelastic scattering, finding that DCS increases when the target absorbs energy and decreases to a minimum before reaching a maximum upon energy emission at specific eV levels [10]. It also increases with the scattering angle. Additionally, the study examines thermodynamic properties of thermal electrons in laser fields, showing variations in thermodynamic energy and potential with field amplitude and temperature [11]. In the case of laser-assisted thermal electron-hydrogen atom elastic scattering, the DCS for thermal electrons was higher than for nonthermal electrons, with interference patterns observed under certain conditions and specific angles [12]. In present work authors trying to interlink DCS with PEMFC performance which help

researcher/reader for thermal management of PEMFC generated during chemical reaction and interaction between the particles formed during chemical reaction at surface of PEMFC electrode.

A PEMFC is a device that converts chemical energy into electrical energy through an electrochemical reaction between hydrogen and oxygen. It consists of an anode, where hydrogen molecules are split into protons and electrons, and a cathode, where oxygen combines with protons and electrons to form water. The protons pass through a polymer electrolyte membrane, while the electrons travel through an external circuit, generating electricity. The overall reaction produces water and heat as byproducts. The reaction around electrode form electron, proton and residue hydrogen which interacts and effects the performance of PEMFC and these electron and proton are causing production of current studied. Dhobi et al. study the DCS around electrode of PEMF and its impact on performance of PEMFC [13-15].

Despite extensive research on fuel cells and scattering phenomena, the integration of scattering principles with technological applications, particularly in PEMFCs, remains underexplored. This work aims to bridge this gap by investigating the relationship between differential cross-section (DCS) variations in weak laser fields and the performance of PEMFCs. By studying the interactions of electrons and protons around PEMFC electrodes, this research seeks to develop a comprehensive understanding of how scattering impacts the efficiency and functionality of PEMFCs, potentially extending these insights to other technological fields.

2 METHODS AND MATERIALS

2.1 Interrelation of S-Matrix and T-Matrix with Amplitude

S-matrix is a matrix element of time development operator $\tilde{T}(t, t_0)$ between unperturbed asymptotic in and out state and denoted by s or *S*. T-matrix is defined in terms of matrix element S-matrix when time tends to $-\infty$ to $+\infty$ whereas transition amplitude is the matrix element of T-matrix in a fixed time and given by [16, 17] as,

$$(S-1)_{fi} = -\frac{i}{\hbar}\int_{-\infty}^{t}\left(\Phi_f V \Psi_i\right) \mathrm{d}t \tag{1}$$

Here $\Phi_f = \phi_f(\boldsymbol{r}) \exp\left(-\frac{iE_f t}{\hbar}\right)$ and $\Psi_i = \psi_i(\boldsymbol{r}) \exp\left(-\frac{iE_i t}{\hbar}\right)$ substituting the value of Φ_i and Φ_f in Eq. (1) and using delta function, we get

$$(S-1)_{fi} = -2\pi i \delta\left(E_f - E_i\right) T_{fi} \tag{2}$$

Here $T_{fi} = \int \phi_f V \psi_i d^3r$ and defined as *T* matrix and $(S-1)_{fi}$ is and transition amplitude. For Elastic scattering there is no change in energy, therefore, the initial and final energy are equal and hence Eq. (2) become

$$(S-1)_{fi} = -2\pi i T_{fi} \tag{3}$$

This equation defines the t-matrix in terms of s-matrix elements of the S-matrix at an infinite time with scattering potential which is time-independent and equal to the Hamiltonian of a system.

2.2 Derivation of S-Matrix and Scattering Amplitude in Terms of the Transition Matrix

Consider a complete set of states $\{\Psi\}$ that satisfy the Schrodinger equation describing the atomic electron that may be in interaction with a laser beam.

$$\frac{i\partial\Psi}{\partial t} = H\Psi = (H_0 + H_I)\Psi \tag{4}$$

Since no laboratory experiment is possible to measure the outcome of an experiment in the laser field. So, as far as laboratory instruments are a concern, there is a complete set of status $\{\Phi_n\}$ that satisfy the Schrodinger equation describing an atomic electron that may be undisturbed or in interaction of the laser field.

$$\frac{i\partial\Phi}{\partial t} = H_0\Phi \tag{5}$$

Hypothetically, the laser pulse is finite, so

$$\lim_{t\to\pm\infty}[H(t) - H_0] = 0 \tag{6}$$

Then, the two complete sets of Φ states and Ψ states can be organized so that correspond at $t \to -\infty$

$$\lim_{t\to-\infty}[\Phi_n(t) - \Psi_n(t)] = 0 \tag{7}$$

After the laser interaction has been introduced, the only wave for the laboratory instrument to discover what has happened is to form an overlap of all possible final Φ_f state with the initial particular state Ψ_i. This forms *S*-matrix such as

$$S_{fi} = \lim_{t\to+\infty}(\Phi_f, \Psi_i) \tag{8}$$

Now the transition matrix, before and after scattering is obtained with the help of *S*-matrix can be obtained as

$$M_{fi} = (S-1)_{fi} = \lim_{t\to+\infty}(\Phi_f, \Psi_i) - \lim_{t\to-\infty}\left(\Phi_f, \Psi_i\right) \tag{9}$$

This is now in the form of an exact differential and represented as

$$M_{fi} = \int_{-\infty}^{\infty}\left(\frac{\partial\Phi_f}{\partial t}, \Psi_i\right)\mathrm{d}t + \int_{-\infty}^{\infty}\left(\Phi_f, \frac{\partial\Psi_i}{\partial \mathrm{t}}\right)\mathrm{d}t \tag{10}$$

Now using Eqs. (4) and (5), we get $\frac{\partial\Phi_f}{\partial t} = -iH_0\Phi_f$ and $\frac{\partial\Psi_i}{\partial \mathrm{t}} = -i(H_0 + H_I)\Psi$ and using these on Eq. (10) we get,

$$M_{fi} = -i\int_{-\infty}^{\infty}\left(\Phi_f, H_{\mathrm{I}}\Psi_i\right)\mathrm{d}t \tag{11}$$

Where H_I is a weak interaction field, since $(S-1)_{fi}$ is a transition amplitude then transition probability per unit time is given with the help of Eq. (2) as

$$W = \lim_{\tau\to\infty} \frac{|(s-1)_{fi}|^2}{\tau} = \frac{1}{\tau}\left(\lim_{\tau\to\infty} \int_{-\frac{\tau}{2}}^{\frac{\tau}{2}} \exp\left[\frac{i(E_f-E_i)t}{\hbar}\right] \frac{\mathrm{d}t}{\hbar} \times \lim_{t\to\infty} \int_{-\frac{\tau}{2}}^{\frac{\tau}{2}} \frac{\mathrm{d}t}{\hbar} \left|T_{fi}\right|^2 \right) \quad (12)$$

Now applying the delta property of delta function and solving we get,

$$W = \left(\frac{2\pi}{\hbar}\right) \delta\left(E_f - E_i\right) \left|T_{fi}\right|^2 \quad (13)$$

For transition into the continuum of final states. The total transition rate in the range $\left(E_f - \frac{\Delta E}{2}\right)$ to $\left(E_f + \frac{\Delta E}{2}\right)$is given by

$$W = \left(\frac{2\pi}{\hbar}\right) \int_{\left(E_f-\frac{\Delta E}{2}\right)}^{\left(E_f+\frac{\Delta E}{2}\right)} \mathrm{d}E \;\; \delta\left(E_f - E_i\right)\left|T_{fi}\right|^2 \rho(E) \quad (14)$$

Here $\rho(E)$ is the density of the final state and on solving Eq. (14) we get,

$$W = \left(\frac{2\pi}{\hbar}\right) \left|T_{fi}\right|^2 \rho(E) \quad (15)$$

2.3 Differential Cross-Section in Born Approximation for Yukawa Potential (YP)

Yukawa purposed potential in 1935 [18] as effective non-relativistic potential which described the strong interactions between nucleons as

$$V(r) = \frac{Ae^{-\mu r}}{r}\; A, \mu > 0 \qquad \text{In Atomic Unit} \quad (16)$$

Here A described the strength of interaction (special case equal to 1), μ is screening parameters (ranges from 0.10 to 1 in bounded case) [1] and $1/\mu$ is its range. This potential is also called Debye-Huckel potential in plasma physics, while this potential also represents as a potential of a charged particle in a weakly nonideal plasma, as well as in electrolytes and colloids, in solid-state as Thomas-Fermi potential. Pais and Jost shows 3D spherical potential such that $I = 2m\int_0^\infty dr r|V(r)|$ is finite for the bounded state is greater than unity. Since amplitude is defined by born first approximation as,

$$f_k(\theta) = -\frac{2m}{k\hbar^2} \int_0^\infty \mathrm{d}r\; r\, V(r) \sin(Kr) \quad (17)$$

Now from Eqs. (17) and (16) we get

$$f_k(\theta) = -\frac{2m_m A}{K\hbar^2} \int_0^\infty \mathrm{d}r\; e^{-\mu r} \sin(Kr) = -\frac{2m_m A}{\hbar^2(\mu^2+K^2)} \quad (18)$$

Here $K = 2k\sin\left(\frac{\theta}{2}\right)$ and m_m is meson mass. Since scattering amplitude is directly proportional to the differential cross-section. Therefore, DCS for YP in the Born approximation is equal to

$$\left(\frac{\mathrm{d}\sigma}{\mathrm{d}\Omega}\right)_{B1}^{Y} = \left[\frac{2m_m A}{\hbar^2\left(\mu^2+4k^2\sin^2\left(\frac{\theta}{2}\right)\right)}\right]^2 \quad (19)$$

In terms of energy, the above Eq. (19) [19, 20] become

$$\left(\frac{\mathrm{d}\sigma}{\mathrm{d}\Omega}\right)_{B1}^{Y} = \left[\frac{2m_m A}{\left(\hbar^2\mu^2+8m_m^2E^2\sin^2\left(\frac{\theta}{2}\right)\right)}\right]^2 \quad (20)$$

Here $E = \frac{\hbar^2k^2}{2m}$ and Eq. (20) gives the DCS in Born approximation with Yukawa potential. This is the case which we considered around electrode in absence of non-monochromatic wave form around electrode due to self-generated case wave due to scattering. This case is considered initial case of collision because at initial state of reaction the speed of particle formed around electrode is higher which increase the energy of electron. In addition, after time pass the number of electrons-proton formation is higher and the effect of screening is also observed around which may affect the flow of electron and decrease the current of PEMFC

2.4 Differential Cross-Section in Born Approximation for Coulomb Potential (CP)

For Coulomb/central potential is defined as $V(r) = \frac{Z_1Z_2e^2}{4\pi\epsilon_0 r} = \frac{A}{r}\; i$n atomic unit, therefore from Eq. (17) the born first amplitude for CP around electrode of PEMFC become

$$f_k(\theta) = -\frac{2mA}{k\hbar^2}\int_0^\infty \mathrm{d}r\; \sin(Kr) = -\frac{2m_eA}{k\hbar^2K} \quad (21)$$

Similarly, as above the DCS in Born approximation for CP obtained with the help of Eq. (21) [19, 20] is

$$\left(\frac{\mathrm{d}\sigma}{\mathrm{d}\Omega}\right)_{B1}^{C} = \frac{m_e^2A^2}{16E^2\sin^4\left(\frac{\theta}{2}\right)} \quad (22)$$

Eq. (22) is similar to the Rutherford formula with the incidence kinetic energy of particles E. For larger momentum transformation that is k^2 is larger a sharp peak is obtained at a small scattering angle ($\theta \to 0$), while at a larger scattering angle ($\theta \to \infty$) the $4k^2\sin^2\left(\frac{\theta}{2}\right)$ is larger. The Born approximation is valid with higher incidence energy of particles in weak scattering potentials. This means the average interaction energy between the incident particle and the scattering potential is much smaller than the incidence kinetic energy of the particle. Also, this case is considered around fuel cell electrode when coulomb potential plays an important role around due to large number of electrons protons formed around electrode of fuel cell.

2.5 Differential Cross-Section in Born Approximation for Square Well Potential (SWP)

SWP in 3D for scattering is defined as

$$V(r<a)=V_0 \\ V(r>a)=0 \tag{23}$$

Now to calculate the born first amplitude, for DCS we have from Eq. (17) and (23)

$$f_k(\theta)=-\frac{2mV_0}{k\hbar^2}\left[\frac{\sin(ka)-ka\cos(ka)}{k^2}\right] \tag{24}$$

Similarly, as above the DCS in Born Approximation for SWP in 3D with the help of Eq. (24) is

$$\left(\frac{\mathrm{d}\sigma}{\mathrm{d}\Omega}\right)_{B1}^{SWP}=\left(\frac{2mV_0}{\hbar^2k}\right)^2\begin{cases}\frac{1}{9}\left(1-\frac{1}{5}k^2a^2\right) & \text{For low Eenergy } (E), ka<1\\ \frac{a^2}{k^2} & \text{For High Energy } (E), ka>1\end{cases} \tag{25}$$

Here m is the mass of considering particle in the potential well. For X-ray scattering with a neutron, the scattering cross-sections are about 10^{-24}cm^2 with the cross-sectional area per atom is about 10^{-16}cm^2 [3]. The potential define in this work is based on the atomic unit with screening parameters unit a_0^{-1} (Bohr's radius) [21]. This is another case scattering case below to condition of equation (23) around electrode inside PEMFC.

In a theory that combines both quantum and relativity theory, it is not possible to specify the position of individual particles precisely. If this is done, in field theory, one has to put off with mathematical inconsistencies which are, indeed, the main problem in quantum field theory. S-matrix theory bypasses this problem by specifying the momenta of the particles. The important new concept theory is the shift of emphasis from object to the event; its basic concern is not with the particles but with their reactions. Such a shift from object to event is required both by quantum theory and relativity. In S-matrix theory, as in field theory, the interaction forces are associated with particles but the concept of virtual particles is not used. Instead, the relation between forces and particles is based on a special property of S-matrix i.e. known as a crossing.

3 RESULTS AND DISCUSSION

The DCS in Born Approximation with Coulomb potential, Yukawa potential and Square Well Potential are studies at different incidence energy of the electron, angle and screening parameters. Taking three cases of around the electrode of PEMFC and help to improve the efficiency of PEMFC knowing the interaction region of particles around electrode my minimizing the space between gas diffusion laser, electrodes and proton exchange membrane. This may help in improve of current state of efficiency [22].

3.1 DCS in Born Approximation for YP

The DCS is based on the atomic unit for meson particle mass $273m_e$ where m_e is a mass of the electron. It is the case if meson formed around the electrode due to scattering between particles around electrode of PEMFC. To study the DCS with scattering angle for YP the screening parameters $0.05a_0^{-1}$, interaction potential strength 1 a.u. and energy of incidence electron 500 a.u. From Fig. 1, it is observed that the scattering at a low angle is high and uncontrollable around the electrode of PEMFC so to control this angle also play an important role and hence to designed PEMFC with flow of inlet fuel angle also play an important role. In addition, this make systems stable which is major challenges [23] of PEMFC.

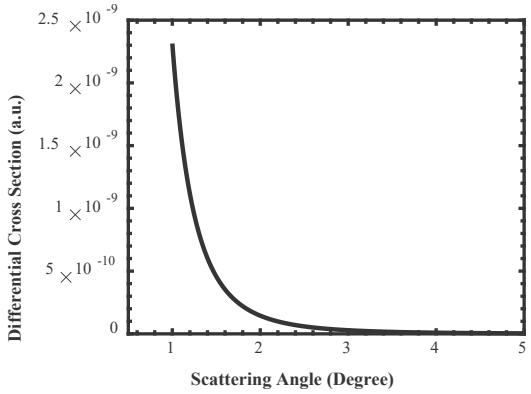

Figure 1 Scattering Angle vs DCS for YP around electrode of PEMFC

But with increasing the scattering angle the scattering goes decrease and become constant at a larger angle [24] but they study for CF_4 like molecules. Because at the large-angle the interaction between target and incidence is less therefore the DCS at large angle is small and constant so this angle may be fit for stable system for PEMFC.

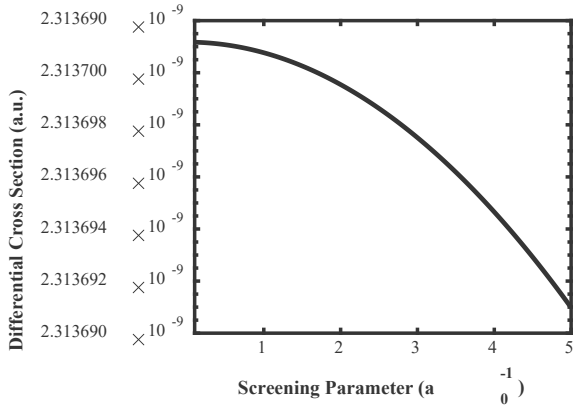

Figure 2 Screening Parameters vs DCS for YP around electrode of PEMFC

Fig. 2, show the effect of screening on DCS as we discussed the continues inlet of hydrogen form screening around the electrode and disturbance of flow of electron effect the performance of PEMFC. Therefore, this study show screening effect DCS and for a system stable lower screening region is best with higher DCS as shown in figure. The observation of DCS with scattering parameters shows the DCS decrease with the increase of screening parameters. In this case, the DCS has no such drastic change in numerical value because with increasing the screening parameters the interaction between target and electron becomes less.

Fig. 3 shows the nature of DCS in Born approximation for YP, with increasing the incidence energy of the electron to target the DCS decrease [25] but they study for He-atom. This is because at high energy of incidence the probabilities of interaction between target and incidence are low as well as target can't see the incidence at high energy. Fig. 3 is for meson incidence particles with mass $273m_e$ at one degree. This also shows that speed of electron corresponding energy effect the DCS and DCS is stable in higher energy region and hence at initial case the seep of particle is higher and performance of PEMFC is higher at initial case than after some time. So, for stable and performance as initial condition DCS management of scattering help the improvement of PEMFC.

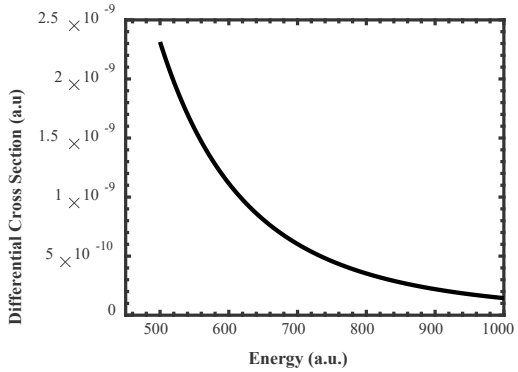

Figure 3 Incidence Energy vs DCS for YP around electrode of PEMFC

The DCS with incidence energy (500 to 1000 a. u.) of meson was ranges from 10^{-10} to 10^{-9} a. u. with 1 degree of scattering angle. The DCS with screening parameters was of the order 10^{-9} a. u. with 1 degree of scattering angle and 500a. u. incidence energy of meson. The DCS with scattering angle was ranges 10^{-10} to 10^{-9} a. u. with incidence energy of meson 500 a. u. for all DCS of YP potential strength is constant as 1 a. u.

3.2 DCS in Born Approximation for CP

Considering the case of scattering around the electrode of PEMFC the DCSC with energy of electrons show decrease as shown in Fig. 3 but for CP the DCS is higher than YP. This observation also shows that at higher energy range the system is stable hence its better knowledge how that DCS nature is for stable system of PEMFC. The DCS in Born approximation for CP was shown in Fig. 4. The observation shows that DCS is decreased with increasing incidence energy of electron with potential strength 1 a.u. at a scattering angle of 1 degree.

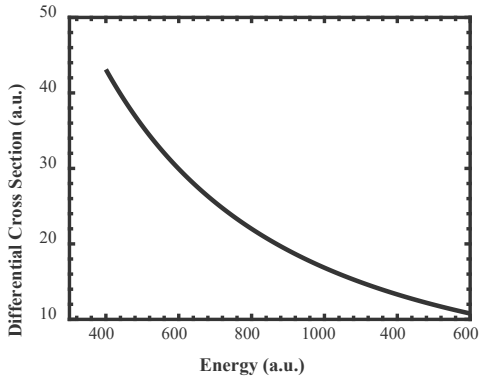

Figure 4 Energy of incidence particles vs DCS for CP around electrode of PEMFC

Similarly, the DCS with scattering angle was also observed as shown in Fig. 5. The observation shows that the DCS is high and uncontrollable/undetectable at a small angle and with increasing the scattering angle the DCS becomes constant, similar to the DCS of YP.

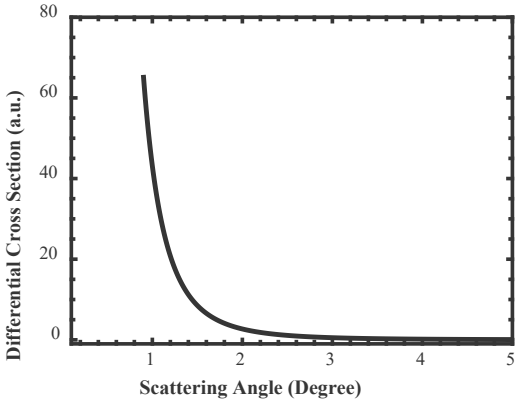

Figure 5 Scattering Angle vs DCS for CP around electrode of PEMFC

The DCS in Born approximation for CP ranged from 10 a. u. to 45 a. u. but the nature is quite different because DCS with scattering angle is sharply decreased while DCS with energy is slow. This case also shows that DCS is stable for higher scattering angle system as YP case. In compare the DCS and stable for PEMFC CP is better than YP case.

3.3 DCS in Born Approximation for SWP

The DCS in Born approximation for SWP is shown in Figs. 6 and 7 respectively from electron and meson. If we considered case around the PEMFC of particle dividing two cases, low (for time passes of reaction) and high energy (initial reaction and formation of particle). The DCS at low energy for the electron is almost zero at momentum 0.5 a. u., potential strength 1 and potential good width 0.9 Å but at high energy DCS goes decrease with increasing scattering angle at momentum 1 a. u. and potential good width 2 Å at same potential strength. The DCS at low energy for meson is almost zero at momentum 0.5 a. u. and potential strength 0.9

a.u. but at high energy, DCS goes decrease with increasing scattering angle at momentum 1 a.u. and potential strength 2 a.u. The DCS when the electron is welling in the potential region is shown in Fig. 6, while meson is in Fig. 7. The DCS for electron was observed up to 200 a.u. while for meson 1.4×10^8 a.u. at high energy of incidence of particles to the target.

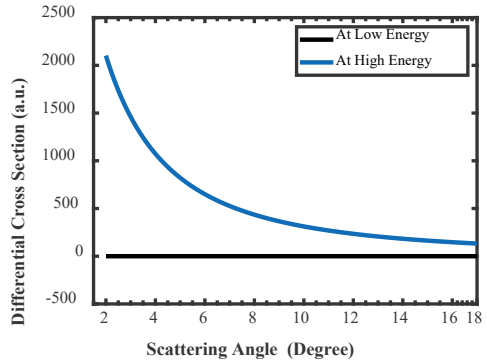

Figure 6 Scattering Angle vs DCS for SWP with the electron as welling particle in Potential Well around electrode of PEMFC

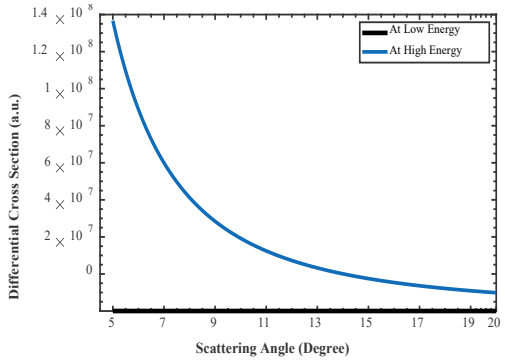

Figure 7 Scattering Angle vs DCS for SWP with meson as welling particle in Potential Well around electrode of PEMFC

On comparing the DCS Fig. 6 and Fig. 7, we can say that at lower energy a constant DCS is observed which means more stable with increasing scattering angle while at higher energy DCS decrease with increasing scattering angle and remain constant at higher scattering angle. In other hand, for stable system at higher and lower energy both are suitable but for complexity on measurement higher DCS is easy. So, the DCS of higher energy in higher scattering angle region is suggested better to design the PEMFC for thermal managements for higher performance.

4 CONCLUSIONS

The DCS in Born Approximation with Coulomb potential, Yukawa potential, and Square Well Potential are also studies with different incidence energy of electron and meson, angle, and screening parameters form around the electrode of PEMFC. The DCS for meson in YP at 1 degree was observed 10^{-10} to 10^{-9} a.u., for an electron in CP, was observed 10 a.u. to 65 a.u. for the electron in SWP was observed up to 2000 a.u. while for meson in SWP was observed 1.4×10^8 a.u. around electrode of PEMFC. The nature found the stable DCS is best for stable performance of PEMFC.

Acknowledgment

The authors would like to thanks all the faculty members of the Department of Physics, Patan Multiple Campus, Patan Dhoka, Lalitpur-4470, Nepal. Similarly, also thanks University Grant Commission Nepal (UGC Award No.: PhD-80/81-S&T-13) for providing research grant for this work.

5 REFERENCES

[1] Alhaidari, A. D. (2021). Taming the Yukawa potential singularity: improved evaluation of bound states and resonance energies. *ArXiv*. 1-2.

[2] Bhatia, A. K. (2020). Scattering and Its Applications to Various Atomic Processes: Elastic Scattering, Resonances, Photoabsorption, Rydberg States, and Opacity of the Atmosphere of the Sun and Stellar Objects. *Atoms. 8*(4), 1-30. https://doi.org/10.3390/atoms8040078

[3] Blügel, S. (2012). Scattering Theory: Born Series. *Lecture Notes of the 43rd IFF Spring School 2012*, Key Technologies, 33, 1-30.

[4] Bothe, W., & Geiger, H. (1925). Uber das Wesen des Compton effects ein experimenteller Breitrag Theorie der Strahlung. *Zeits für Phys., 32*(1), 639-663. (in German) https://doi.org/10.1007/BF01331702

[5] Compton, A. H. (1923). A Quantum Theory of the scattering of X-rays by light. Elements. *Phys. Rev., 21*, 1-6. https://doi.org/10.1103/PhysRev.21.483

[6] Compton, A. H., & Simon, A. W. (1925). Directed Quanta of Scattered X-rays. *Phys. Rev. 1925*, 26, 3-5. https://doi.org/10.1103/PhysRev.26.289

[7] Savelyeve, I. V. (1981). Physics: A General Course, Vol. III, MRI Publishers Moscow.

[8] Kroll, N. M., Watson, K. M., & Keldysh, L. (1973). Ionization in the field of a strong Electromagnetic wave, *Physical Review A, 20*(5), 1307-1314.

[9] Reiss, H. R. (2010). *High-Field Laser Physics*. ETH, Zürich, Switzerland.

[10] Dhobi, S. H., Nakarmi, J. J., Yadav, K., Gupta, S. P., Koirala, B., & Shah, A. K. (2022). Study of thermodynamics of a thermal electron in scattering. *Heliyon, 8*(12). https://doi.org/10.1016/j.heliyon.2022.e12315

[11] Dhobi, S. H., Gupta, S. P., Yadav, K., Nakarmi, J. J., & Jha, A. K. (2024). Differential Cross Section with Volkov-Thermal Wave Function in Coulomb Potential. *Atom Indonesia, 1*(1), 19-25. https://doi.org/10.55981/aij.2024.1309

[12] Dhobi, S. H., Yadav, K., Jha, A. K., Karki, B., & Nakarmi, J. J. (2022). Free Electron-Ion Interaction and Its Effect on Output Current of Permeable Exchange Membrane Hydrogen Fuel. *ECS Transactions, 107*(1), 8457. https://doi.org/10.1149/10701.8457ecst

[13] Dhobi, S. H., Gupta, S. P., Nakarmi, J. J., Koirala, B., Yadav, K., Oli, S. K., & Gurung, M. (2023). Scattering of Free Electrons with Hydrogen Atoms in Proton Exchange Membrane Fuel Cell System. *International Annals of Science, 13*(1), 22-28. https://doi.org/10.21467/ias.13.1.22-28

[14] Dhobi, S. H., Pudasaini, A., Oli, D., Khatiwada, S., Ghimire, K., Rijal, O. S., ... & Paudel, G. (2024). Scattering of Free Electrons with Hydrogen Atoms in Proton Exchange Membrane Fuel Cell. *Hadronic Journal, 47*(1).

https://doi.org/10.29083/HJ.47.01.2024/SC1
[15] ETH Lecture (2011). *Quantum Mechanics without Perturbation Theory*. Zürich, Switzerland.
[16] Frijof, C. (1976). *The Tao of physics*. 3rd Edition, Harper Collins Publishers, Fulham Palace Road, United Kingdom.
[17] Liverts, E. Z., & Mandelzweig, V. B. (2009). Analytical computation of amplification of coupling in relativistic equations with Yukawa potential. *Annals of Physics, 324*(2), 388-407. https://doi.org/10.1016/j.aop.2008.08.004
[18] Collas, P. (2021). Coulomb scattering in the Born approximation and the use of generalized functions. *ArXiv*, 5-6. https://doi.org/10.1119/10.0005453
[19] GUFAM. (2021). Lecture 5: Scattering theory, Born Approximation Born Approximation, SS2011: Introduction to Nuclear and Particle Physics, Part 2.
[20] Nayek, S., & Ghoshal, A. (2012). Dynamics of positronium formation in positron-hydrogen collisions embedded in weakly coupled plasmas. *Phys. of Plasmas, 19*, 1-14. https://doi.org/10.1063/1.4764467
[21] Harper, C. (2006). *Introduction to Mathematical physics, California State University*. Prentice Hall of India Pvt. Ltd, India.
[22] Park, S., & Lee, S. (2023). Theoretical Analysis for Improving the Efficiency of HT-PEMFC through Unreacted Hydrogen Circulation. *Applied Sciences*. https://doi.org/10.3390/app13169292
[23] Chen, L., Xu, K., Yang, Z., Yan, Z., & Dong, Z. (2022). Optimal Design and Operation of Dual-Ejector PEMFC Hydrogen Supply and Circulation System. *Energies*. https://doi.org/10.3390/en15155427
[24] Ketkar, & Bonham (1985). Small-angle elastic differential scattering cross section for 25-keV electrons scattering from helium. *Physical Review Letters, 55*(13), 1395-1397. https://doi.org/10.1103/PhysRevLett.55.1395
[25] Nagashima, Y., Hyodo, T., Fujiwara, K. & Ichimura, A. (1998). Momentum-transfer cross section for slow positronium-He scattering. *Journal of Physics B, 31*, 329-339. https://doi.org/10.1088/0953-4075/31/2/014

Authors' contacts:

Saddam Husain Dhobi
(Corresponding author)
Central Department of Physics, Tribhuvan University,
Kirtipur, Kathmandu-44600, Nepal
Department of Physics, Patan Multiple Campus, Tribhuvan University,
Lalitpur-44700, Nepal
E-mail: saddam@ran.edu.np

Kishori Yadav
Department of Physics, Patan Multiple Campus, Tribhuvan University,
Lalitpur-44700, Nepal

Suresh Prasad Gupta
Department of Physics, Patan Multiple Campus, Tribhuvan University,
Lalitpur-44700, Nepal
E-mail: guptasir@gmail.com

Jeevan Jyoti Nakarmi
Central Department of Physics, Tribhuvan University,
Kirtipur, Kathmandu-44600, Nepal
Department of Physics, Patan Multiple Campus, Tribhuvan University,
Lalitpur-44700, Nepal

Ajay Kumar Jha
Department of Mechanical and Aerospace Engineering, Institute of Engineering,
Tribhuvan University, Pulchowk Campus, Lalitpur, Nepal